Fabrication of Ordered Porous Polymer Film via a One-Step Strategy and Its Formation Mechanism

Shiling Zhang, Shuxue Zhou, Bo You, and Limin Wu*

Department of Materials Science and the Advanced Coatings Research Center of China Educational Ministry, Advanced Materials Laboratory, Fudan University, Shanghai 200433, P. R. China

Received January 11, 2009

ABSTRACT: In this paper, a series of colloidal polymers with various T_g, composition, and sphere size were synthesized by surfactant-free emulsion polymerization and dispersion polymerization methods and then blended with colloidal silica particles to obtain polymer/silica nanocomposite latexes. When these nanocomposite latexes were forced dry at high temperature (e.g., 110 °C) for 2 h, a three-dimensional ordered porous structure was directly obtained. Neither complex processes nor removal of any templates like in a templating method is needed. These ordered pores should form from the top surface and then propagate layer by layer from the top surface to substrate.

Introduction

In the past decade, the strategy to fabricate two- or three-dimensional ordered porous polymer films has attracted considerable attention, since these films have some important potential applications, such as catalytic surfaces and supports,[1] chromatographic materials and filters,[2] lightweight structural materials,[3,5] thermal insulating materials and acoustic damping materials,[4] low dielectric constant materials,[5] and photonic crystals.[6,7]

Generally, the ordered porous materials are mainly fabricated via templating techniques that are based on self-assembly of colloidal spheres (usually silica or polystyrene),[8−10] condensing water droplets,[11−13] surfactants,[14] and block copolymers.[15] In particular, the self-assembly of colloidal spheres is the most widely used strategy due to its relatively high-efficiency, low-cost mass production[16] and because it is especially suitable for the preparation of three-dimensional ordered porous materials with precisely controlled pore sizes.[8,9,17] In this approach, the framework is generally formed by infiltrating a liquid precursor[6,17,18] or nanoparticles[19−21] into the voids among the dried colloidal spheres array and then converting them into the desired solid phase. For example, Schroden et al.[18] infiltrated silica, titania, or zirconia precursors into polymer colloidal spheres array and then got three-dimensional ordered porous structures by calcination or solvent extraction after solidification of the inorganic precursor. Wang et al.[19] filled silica nanoparticles into the voids of the polymer sphere film that was composed of polymer spheres with two particle sizes and pyrolyzed the organic components, leading to a combined structure of mesopores and macropores. However, although the self-assembly of colloidal spheres provides an effective route to ordered porous materials, it suffers from a number of limitations: First, multistep processes, e.g., the assembly of template spheres, the infiltration of fluids, and the solidification of fluids by chemical or physical treatment, are needed for preparation of the template-containing polymer films. Second, in order to obtain the ordered porous films, removal of the templates by etching or calcination processes is usually indispensable. Third, the replicas are easy to crack due to shrinkage involved in solidification and pyrolysis. As a consequence, this strategy lacks the characteristics required for high-volume production in practical application. Therefore, attaining a much simpler and more feasible strategy for fabrication of ordered materials still remains a great challenge for materials scientists.

Table 1. Formulations for Syntheses of Monodisperse Polymer Spheres

runs	HAPS (g)	monomer mixture (g)	particle size[a] (nm)	ζ (mV)	T_g[b] (°C)
1	0.25	BMA/MMA/AA = 20.0/0/1.0	416	−50.1	25
2	0.25	BMA/MMA/AA = 19/1.0/1.0	473	−52.2	30
3	0.25	BMA/MMA/AA = 15.2/4.8/1.0	401	−58.8	40
4	0.25	BMA/MMA/AA = 10.8/9.8/1.0	385	−54.0	63
5	0.25	BMA/MMA/AA = 6.0/14.0/1.0	273	−53.0	85
6	0.25	BMA/MMA/AA = 0/20.0/1.0	269	−51.9	105
7	0	BMA = 10	363	−43.8	
8	0.25	BMA/MMA/HEMA = 17.6/2.4/2.0	530	−60.4	
9	0	St/BA/AA = 12.4/7.6/1.0	584	−61.1	
10	0.25	St/BA/AA = 12.4/7.6/1.0	366	−65.9	
11	0	St/BA = 9.3/5.7 (initiator AIBN)	1300	−26.2	

[a] Determined by dynamic light scattering. [b] Since the measured values of T_g are close to theoretical ones that are far lower than drying temperature (110°C) and have little effect on porous structure, the T_g values for the last six samples are not listed.

Recently, we have developed a novel and facile method that we define as the "forced-drying" strategy for nanocomposite polymer latex to fabricate two- or three-dimensional ordered porous nanocomposite films.[22,23] In this approach, poly(styrene−butyl acrylate−acrylic acid)/colloidal silica nanocomposite latex was first prepared in situ by surfactant-free emulsion polymerization or by blending method followed by forced-drying to form film at comparatively high temperature (e.g., around 100 °C or much higher). It was surprising to find that a two- or three-dimensional ordered porous film can be directly fabricated, respectively. Neither complex processes nor removal of any templates, as in the templating method, is needed; therefore, it is really feasible, inexpensive, and environmentally friendly and can be used for a large-scale fabrication of ordered porous polymer films. In this study, we further investigated the effects of some key parameters, e.g., polymers with various glass transition temperature (T_g), composition, and sphere size, on the formation of ordered porous film, and tried to really understand the formation mechanism of this ordered porous structure via the forced-drying strategy.

Experimental Section

Materials. The monomers methyl methacrylate (MMA), butyl methacrylate (BMA), butyl acrylate (BA), styrene (St), acrylic acid

* Corresponding author. E-mail: lmw@fudan.edu.cn, lxw@fudan.ac.cn.

10.1021/ma900055f CCC: $40.75
Published on Web 04/22/2009

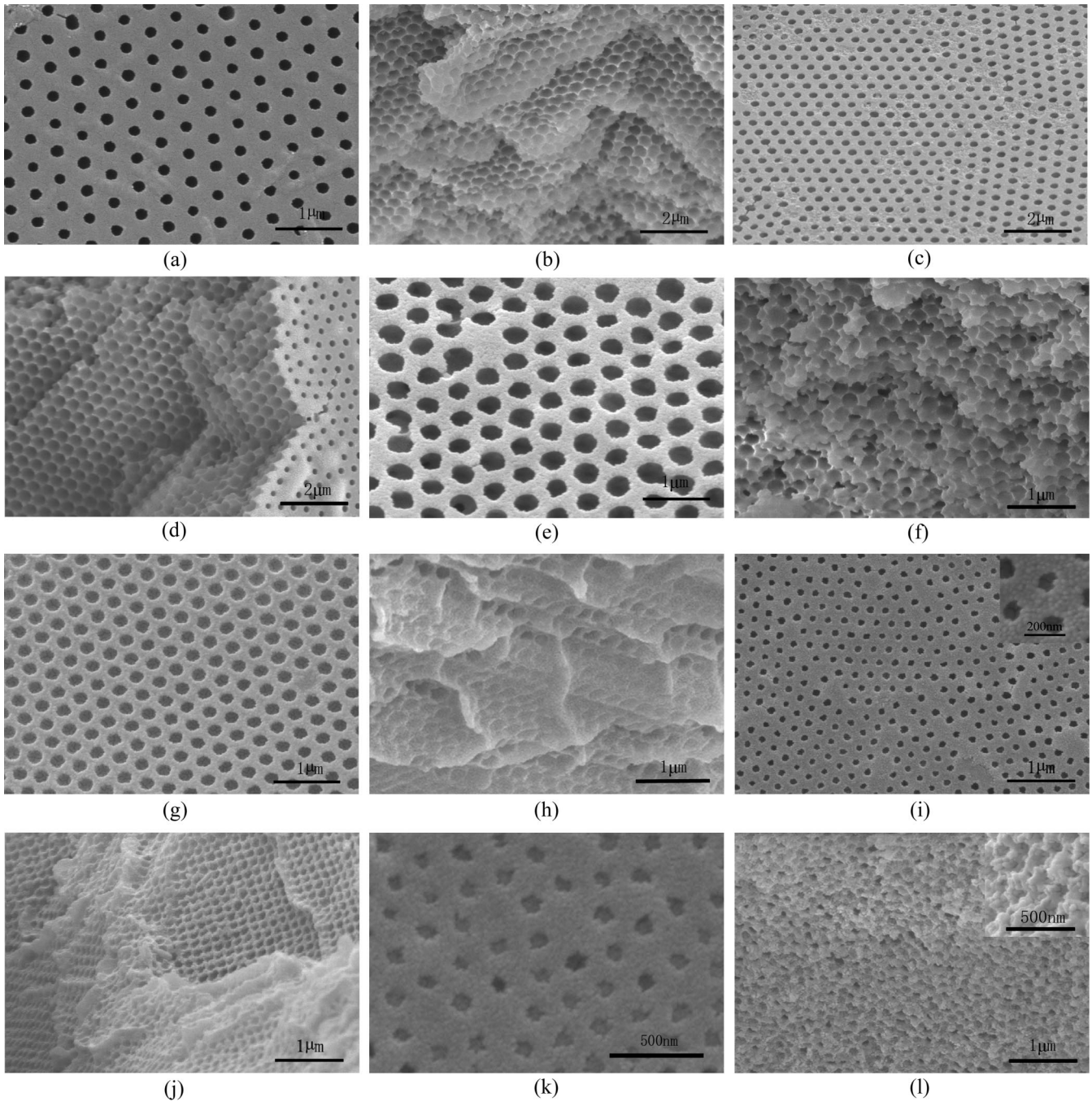

Figure 1. The SEM images of the top surface (left column) and cross section (right column) of the films with various T_g of polymer: (a and b) 25 °C (run 1), (c and d) 30 °C (run 2), (e and f) 40 °C (run 3), (g and h) 63 °C (run 4), (i and j) 85 °C (run 5), (k and l) 105 °C (run 6) (silica sol: 034DI).

(AA), and hydroxyethyl methacrylate (HEMA) were purchased from Sinopharm Chemical Reagent Corp. The auxiliary monomer allyloxy hydroxypropyl sodium sulfonate (HAPS, 40 wt % of solid content in aqueous solution) was kindly donated by Shuangjian Trading Corp. Ltd. The colloidal silicas Bindzil 2034DI (20 nm, pH 3, solid content = 34 wt %, ζ-potential = −11.1 mV) and Nexsil 8 (8 nm, pH 10, solid content = 30 wt %, ζ-potential = −47.1 mV) were provided by Eka Chemicals Corp. and Nyacol Nanotechnologies, Inc., respectively. The initiators 2,2′-azobisisobutyronitrile (AIBN) and ammonium persulfate (APS) were purchased from Shanghai Guanghua Chemical Reagent Corp. and purified by recrystallization. Other ingredients were polyvinylpyrrolidone K-90 (PVP K90), sodium bis(2-ethylhexyl) sulfosuccinate, absolute ethanol, and ultrapure water (>17 MΩ cm^{-1}).

Synthesis of Colloidal Polymer Spheres. Both emulsion polymerization and dispersion polymerization were employed to synthesize the colloidal polymer spheres according to the formulations in Table 1.

The negatively charged polymer spheres from runs 1−10 were synthesized by a semibatch surfactant-free emulsion polymerization. The typical synthetic procedure is described as follows: a certain amount of HAPS solution and 80 g of deionized water were charged into a 250 mL round-bottom flask equipped with mechanical stirrer, thermometer with a temperature controller, an N_2 inlet, a Graham condenser, and a heating mantle, and the mixture was stirred at room temperature for 15 min and 25% of monomers mixture was slowly added within 30 min. This reaction system was deoxygenated by bubbling nitrogen gas at room temperature for ∼1 h and then heated to 80 °C, followed by addition of aqueous APS solution (0.035 g of APS in 3 g of water). This reaction was conducted at 80 °C for 1.5 h under a slow stream of N_2, and then another aqueous APS solution (0.14 g APS in 12 g of water) and the residual

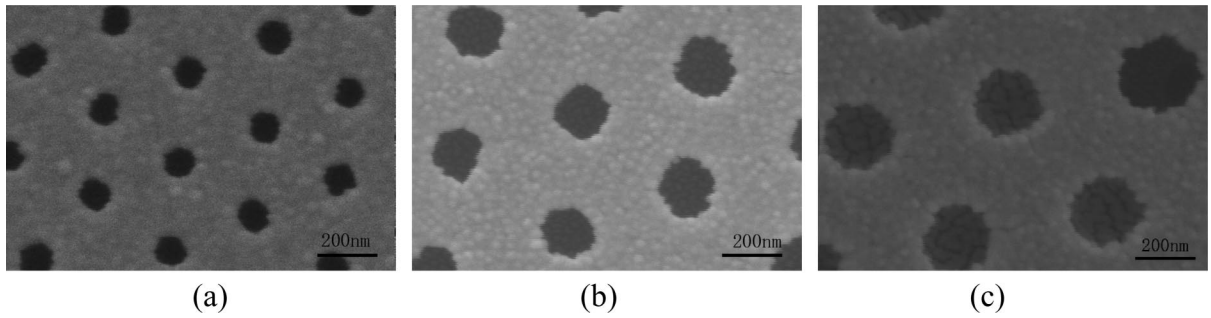

Figure 2. SEM images of the top surface of films with various kinds of monomer: (a) PBMA (run 7), (b) poly(BMA−MMA−HEMA) (run 8), (c) poly(St−BA−AA) (run 9) (silica sol: 2034DI).

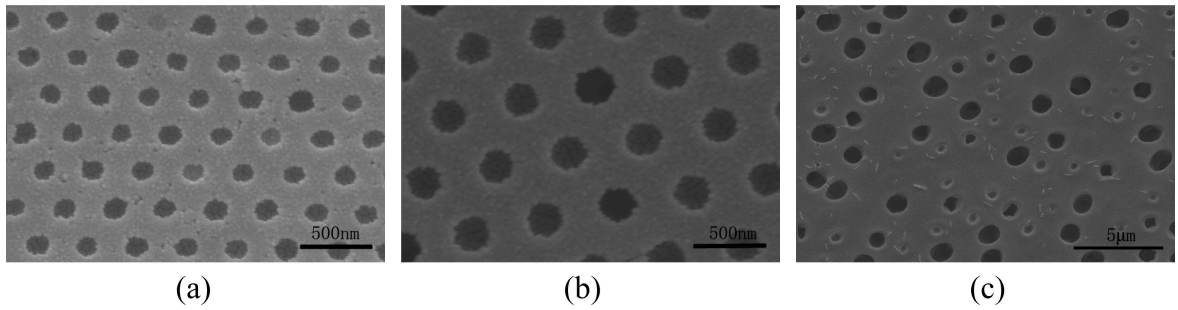

Figure 3. Surface SEM images of the nanocomposite films from different sizes of polymer: (a) 366 nm, (b) 584 nm, (c) and 1300 nm (silica: Nexsil 8, 15 wt % based on polymer).

monomers mixture were over a period of 2 h and continued to react at 80 °C for another 5 h to obtain negatively charged polymer spheres colloids.

The negatively charged polymer sphere in run 11 was prepared by dispersion polymerization: 2.14 g of PVP, 0.5 g of sodium bis-(2-ethylhexyl)sulfosuccinate, 85 g of absolute ethanol, and 15 g of water were sequentially added into a 250 mL four-neck round-bottom flask, and then the mixture was stirred overnight at room temperature, followed by adding a solution of AIBN in monomers. The reactant solution was deoxygenated by bubbling super-purity-grade nitrogen gas at room temperature for 1 h, and then the solution was heated to 70 °C and kept at that temperature for 24 h under a stirring speed of 100 rpm. The obtained suspension was dialyzed against deionized water using a cellulose membrane to obtain big negatively charged polymer spheres with a ζ-potential of −26.2 mV.

Preparation of Ordered Porous Polymer Films. On the basis of our previous forced-drying process,[22,23] the as-prepared polymer latex (or dispersion) was blended with silica sol by magnetic stirring for 1 h to prepare nanocomposite polymer latex and then cast on glass substrates by pouring method. When these substrates cast with nanocomposite polymer latex were directly dried in an oven at 110 °C for 2 h without predrying at ambient temperature, a three-dimensional periodic porous structure was directly obtained.

Characterization. Scanning electron microscopy (SEM) was conducted with a Philips XL 30 field emission microscope at an accelerating voltage of 10 kV. Transmission electron microscopy (TEM) was carried out with a Hitachi H-600 microscope (Hitachi Corp.) operated at 200 kV. X-ray photoelectron spectroscopy (XPS) detection was performed by a Perkin-Elmer PHI 5000 C ESCA system using Al Kα radiation (1486.6 eV) at a power of 250 W. Thermogravimetric analysis (TGA) was analyzed using a TGA Model SDT 2960 apparatus (TA Instruments, New Castle, DE). ζ-Potential of dispersions was determined using a ZetaPlus-ZetaPotential analyzer (Brookhaven Instruments Corp., Holtsville, NY). T_g was determined using a Pyris 1 differential scanning calorimeter (DSC) (Perkin-Elmer, Inc.). Average size and size distribution were measured using dynamic light scattering (DLS, Beckman Coulter Corp.).

Table 2. Summary of Microstructure of Composite Films (before Calcination)

runs	15 wt % silica sol	pore array	center-to-center distance (nm)[a]	pore density on surface[b]
1	2034DI	ordered	440	752
2	2034DI	ordered	470	714
3	2034DI	ordered	375	711
4	2034DI	ordered	370	1223
5	2034DI	ordered	240	2280
7	2034DI	ordered	300	1124
8	2034DI	ordered	518	632
9	Nexsil 8	ordered	520	482
10	Nexsil 8	ordered	320	1088
11	Nexsil 8	disordered	950	56

[a] Elicited from SEM images of two neighboring pores. [b] Number of pores in an area of 10 × 10 μm^2 directly elicited from SEM images.

Results and Discussion

Effect of ζ-Potential. All as-prepared colloidal polymer latexes were diluted with deionized water (the amount of latex and water were same for all samples; pH values were about 6 and 7 for runs 1−10 and 11, respectively) and checked for their ζ-potential, also summarized in Table 1. Just as designed and expected, all the polymer spheres have negatively charged surfaces, stemming from SO_4^-, ionized carboxyl ($-COO^-$), or $-SO_3^-$. When these colloidal polymer spheres were blended with two types of silica sol, all the nanocomposites had more than 1 month of stability except for the mixture of run 11 with 2034DI. This is because both the polymer spheres in run 11 and 2034DI are less negatively charged than those in runs 1−10 and Nexsil 8, respectively, and the weak repulsion between the polymer spheres in run 11 and 2034DI is not enough to stabilize the nanocomposite. If a positively charged polymer colloid was blended with these colloidal silica beads, fast flocculation would happen. These results indicate that a strong electrostatic repulsive force between polymer spheres and colloidal silica beads is indispensable for preparing stable polymer/silica nanocomposites.

Effect of Polymer Composition. A series of colloidal polymer spheres with different T_g were synthesized by varying

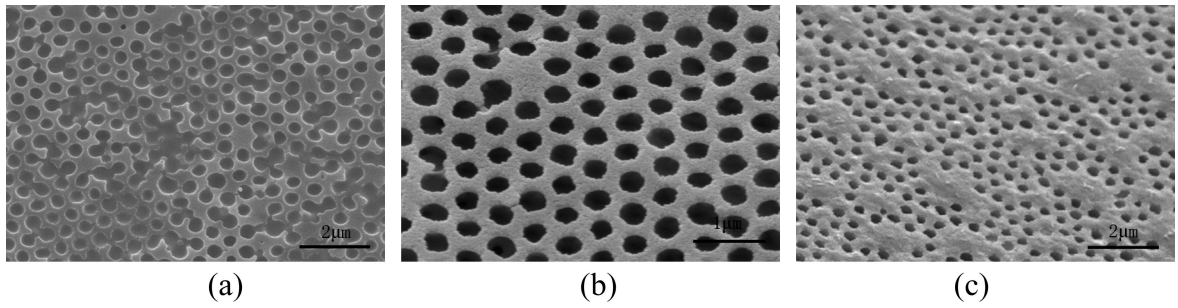

Figure 4. SEM images of the top surface of the film with different silica contents: (a) 7.5 wt %, (b) 15 wt %, and (c) 25 wt %.

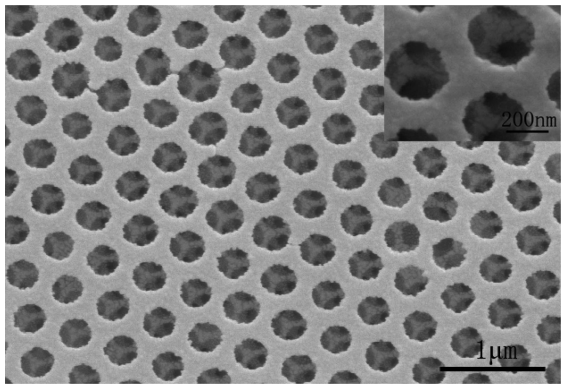

Figure 5. SEM image of composite film after calcination.

BMA/MMA mass ratios (runs 1−6 in Table 1) and then blended with 15 wt % of silica sol to obtain nanocomposite latexes. These latexes were cast on glass substrates and then forced dry at 110 °C for 2 h; the SEM images of the top surfaces and cross sections of these nanocomposite films are demonstrated in Figure 1. It can be seen that all these films exhibit three-dimensional ordered porous structure. Moreover, this structure appears to be typical face-centered cubic (fcc), which can be observed in the (100) plane in Figure 1j, each pore being surrounded by six equal pores in layers perpendicular to the (111) direction. As the T_g of polymer increases from 25 to 30, 40, 63, 85, and 105 °C, the pores become shallower. This should be attributed to the lower chain mobility of the polymer with higher T_g; increasing the drying temperature could probably improve the porous structure of these polymers with high T_g. Polymers with much higher T_g were not investigated because too high a T_g caused a brittle film.

Furthermore, the monomers in the above polymers were replaced by other kinds of monomers to synthesize colloidal polymer spheres with different monomer composition, such as poly(butyl methacrylate) (PBMA), poly(BMA−MMA−HEMA), poly(St−BA−AA) (runs 7−9), which were then blended with 15 wt % of silica sol and forced dry at 110 °C for 2 h. The SEM images of both surfaces and cross sections, shown in Figure 2, display that all the films also show three-dimensional ordered porous array. Combining Figures 1 and 2, it can be concluded that the forced-drying strategy, which was developed recently,[22,23] can be employed to fabricate periodic porous polymer films with different compositions.

Effect of the Size of Polymer Spheres. Figure 3 illustrates the surface SEM images of the nanocomposite films prepared from 366, 584, and 1300 nm polymer spheres (runs 10, 9, and 11, respectively) by forced-drying at 110 °C for 2 h. The nanocomposite films from 366 and 584 nm polymer spheres reveal an ordered porous structure (Figure 3a,b) while the film with 1300 nm polymer spheres had a randomly porous structure (Figure 3c). Table 2 further summarizes the center-to-center distances between neighboring pores and the pore density of the three samples and other nanocomposite films. In comparison with the particle sizes of the polymers listed in Table 1, it is interesting to see that the center-to-center distances between two neighboring pores are very close to the original sizes of the corresponding polymer spheres, and the smaller the polymer spheres are, the larger the pore density is. This suggests that the three-dimensional ordered pores should come from the colloidal polymer spheres, and the porous size and density can be controlled by the polymer sphere size. However, too big monodisperse polymer spheres, e g., run 11, may be harder to self-assemble and would lead the three-dimensional pore structure to be disordered, probably because the larger spheres are harder to move.

Effect of Silica Content. Figure 4 further demonstrates the typical SEM images of the nanocomposite films with various nanosilica contents. At 7.5 wt % silica sol, shallow and interconnected pores are clearly seen on the film surface (Figure 4a), and these pores are somewhat orderly arrayed. This could be due to the insufficient silica particles for formation of an integrated silica framework. As silica sol was increased to 15 wt %, regular ordered porous structure can be obtained (Figure 4b). As the silica content was further increased to 25 wt %, pores could be seen but are locally distributed on the planar surface (Figure 4c). These results suggest that 25 wt % silica sol is already in excess for an integrated silica framework.

Theoretically, the volume fractions of polymers and voids in fcc crystal packing structure are 74% and 26%, respectively. If the voids are completely filled with silica nanoparticles based on fcc structure, the volume fraction of silica would be 19.2% in the voids of colloidal polymer crystal, corresponding to a weight fraction of 48.8 wt % based on the weight of polymer (assuming that the densities of polymer and silica beads are 1.17 and 2.2 g cm^{-3}, respectively). However, in our cases, 15 wt % of silica is already enough to form three-dimensional ordered porous structure, suggesting that silica beads are actually loosely packed in the voids. Thus, it could be calculated that about 20 vol % of voids remain in the whole film when 15 wt % of silica filled in the fcc colloidal polymer crystal.

Composition of the Ordered Porous Film. The typical ordered porous film was scanned and analyzed by XPS, and it was found that the atomic ratio of Si:C at the film surface was 1.55:77.9, far lower than their theoretical ratio (4.07:77.9). This indicates that the top layer of the film surface is enriched in polymer chains, since polymer has lower surface free energy than nanosilica. TGA analysis of the typical porous film shows 7.1% below 300 °C and 78.9% at 300−450 °C, corresponding to the evaporation of physically adsorbed water and the decomposition of polymer, respectively; the char yield is 14.0%, which is consistent with the theoretical content of silica. This porous film was further calcinated at 500 °C for 3 h to remove polymer completely and scanned by SEM, and it can be seen

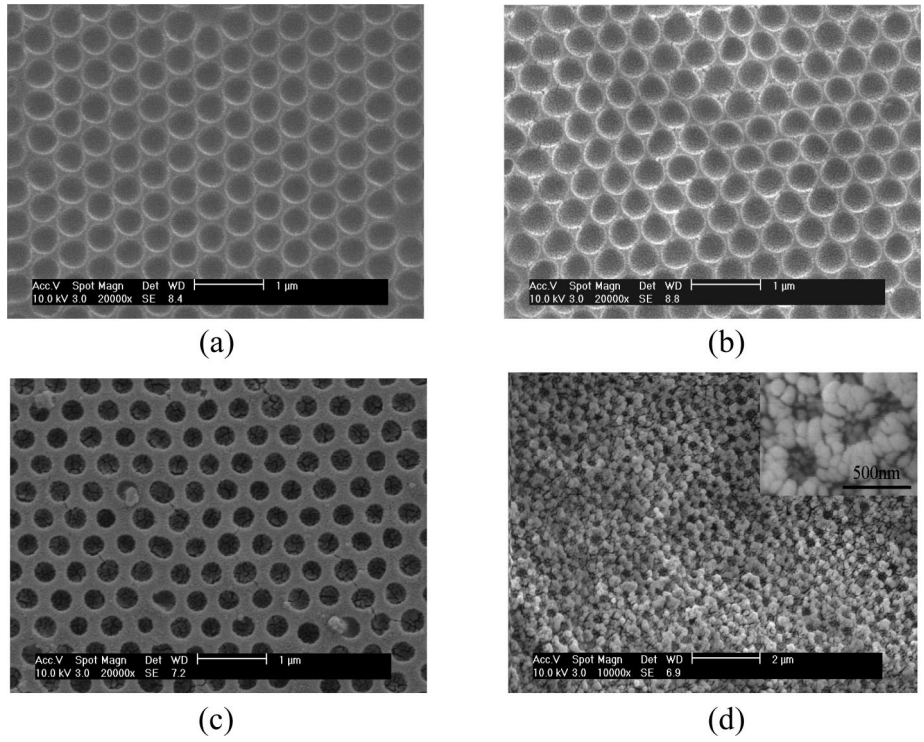

Figure 6. SEM images of (a) the top surface of the composite film dried at 60 °C, (b) the top surface of the composite film dried at 60 °C for 2 h and then at 110 °C for another 2 h, (c) the top surface of the composite film dried at 60 °C and then immersed into water and dried at 110 °C, and (d) cross-section of the composite film dried at 60 °C.

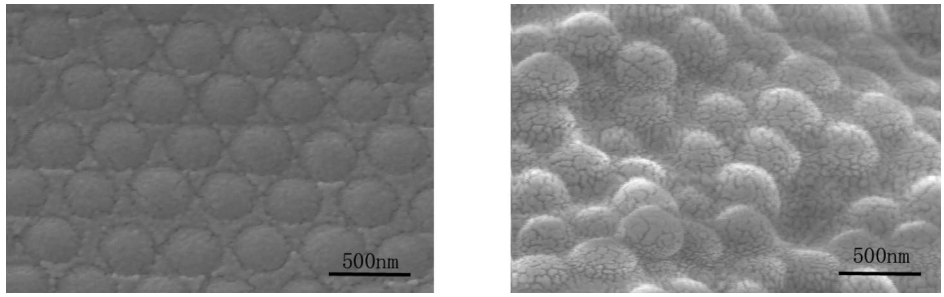

Figure 7. SEM images of the top surface (left) and cross-section (right) of films from the cross-linked polymer spheres.

that three-dimensional macropores are interconnecting by uniform windows, as indicated in Figure 5. This confirms that the silica particles constitute the three-dimensional framework.

Formation Mechanism of the Ordered Porous Film. In the typical self-assembly of colloidal crystal method, the polymer sphere templates are removed by calcination or dissolution to fabricate a two-dimensional or three-dimensional ordered porous film. However, in our forced-drying strategy of nanocomposite latex, neither calcination nor dissolution was employed. Then, how does this ordered porous structure form? What are the driving forces to form the ordered porous structure? Where have the polymer spheres gone, since these pores are coming from polymer spheres?

Generally, there are three drying modes for a wet film:[24] The first one is the homogeneous drying mode, that is, the water concentration is spatially homogeneous in the film and all parts of the film dry at the same rate. In the second mode, the evaporating liquid concentrates the particles at the liquid−air interface, resulting in a sheet of packed particles at the surface of the film, and the packed regions grow in thickness as the vertical convection induced by the capillary pressure draws more particles into the region. The third mode involves lateral front propagation, and the particles concentrate first at the edges. To understand which drying mode the wet composite film follows, two kinds of conditions were employed to dry the wet composite film: the wet composite film was dried at 60 °C for 2 h, followed either by drying at 110 °C for another 2 h or by immersion into water and drying at 110 °C for 2 h. Figure 6 presents the SEM images of these composite films treated under various conditions. It can be seen that both the composite film dried at 60 °C and the film first dried at 60 °C and then 110 °C show very similar morphology (see Figure 6a,b). However, as the film dried at 60 °C was then immersed into water and further dried at 110 °C, the film displays deeper pores on the surface, and the width of boundary between two pores becomes larger compared with the films first dried at 60 °C and then 110 °C (see Figure 6c). The cross-section of the composite film dried at 60 °C shows irregular spherical and smaller pores (see Figure 6d) than the film directly dried at 110 °C, as shown in Figure 1d. Just discussed above, there exist some voids in polymer crystal and loosely packed silica beads, and immersion in water can promote the mobility of polymer chains into these voids to form deeper porous structure. A control experiment with the cross-linked polymer spheres to replace the linear polymer spheres shows

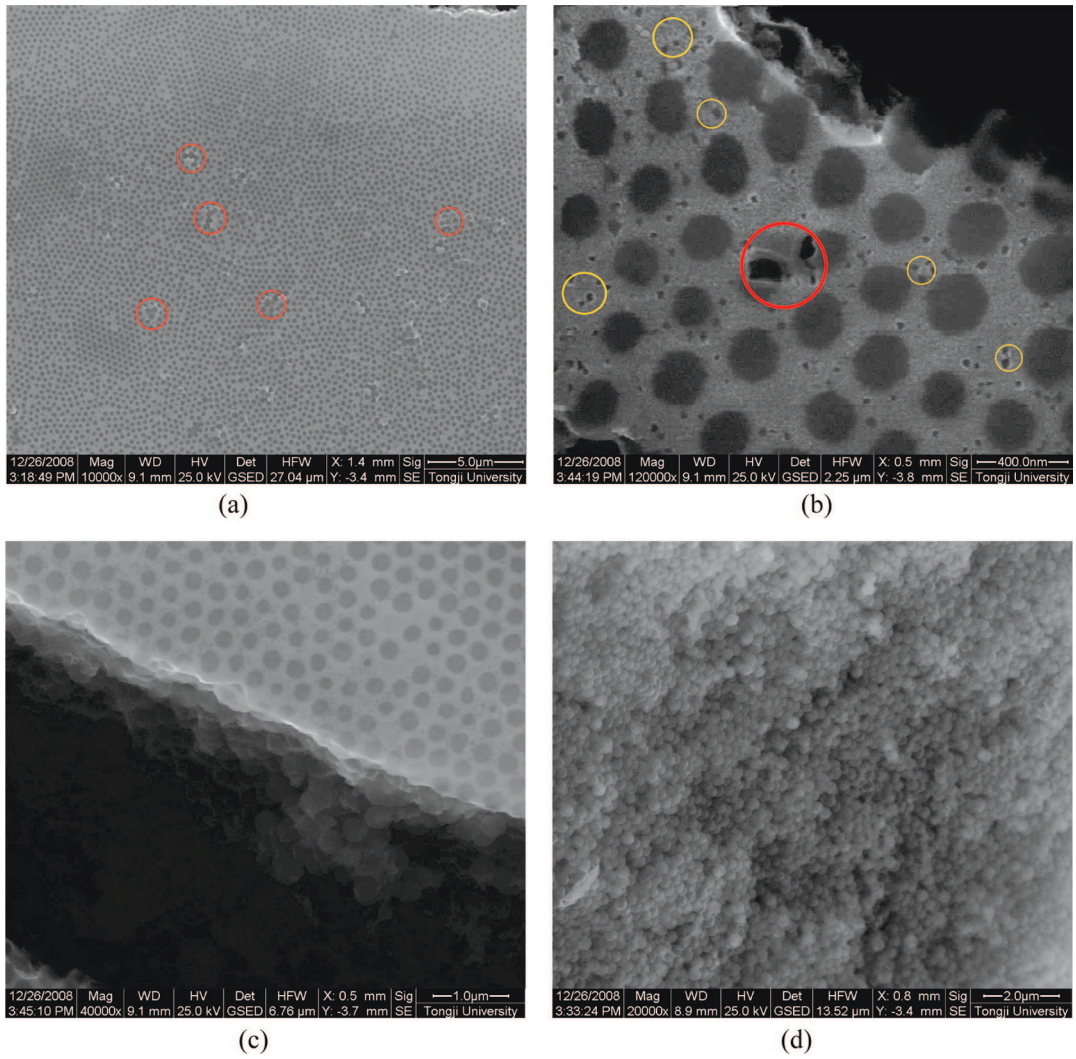

Figure 8. SEM images of the composite film dried at 110 °C for 10 s and treated by vacuum at 0 °C: (a) the top surface, (b) an amplified image of the top surface, (c) cross-section of the film, and (d) the bottom surface.

no porous structure, as shown in Figure 7. These results further confirm that the mobility and diffusion of polymer chains are absolutely necessary for forming the ordered porous structure.

Another experiment involves the wet composite film dried at 110 °C for 10 s with its water then immediately removed by vacuum at 0 °C and observed by SEM. It is found from Figure 8 that the top surface of the composite film has already consolidated even though it was dried at 110 °C for only 10 s, and the porous structure is forming on the surface (see Figure 8a). More careful observation from the amplified image displays that a thin top layer is also covering the porous structure (see Figure 8b, the red circle refers to artificially broken parts of the film), no pores are observed along the direction perpendicular to the substrate, and on the bottom (see Figure 8c,d), the black particles on the top surface should be silica beads (indicated by yellow circles in Figure 8b). These results suggest that the drying process of the composite film is following the second mode, namely, the drying starts from the top surface to the bottom.

On the basis of all the experimental results and discussion, a possible formation mechanism of three-dimensional ordered porous film is deduced and schematically described by Figure 9. As water evaporates, the concave capillary bridge between particle pairs, e.g., polymer spheres and silica particles, plays a significant role in pulling the particles together in order, while conventional colloidal forces such as electrostatic repulsion forces grant mobility to the spheres during the assembly.[25] Thus, the monodisperse polymer spheres self-assemble quickly into colloidal crystal fragments[26] that then impinge to form the first continuous layer of the ordered packed structure on the top surface. Simultaneously, the small silica beads are transporting through channels among the spheres in the consolidated layer to the evaporating menisci at the surface and accumulating and filling in the interspaces between spheres, as shown in Figure 9b. On another hand, since the polymer has a far lower surface free energy (37.6 mJ/m^2) than silica (103.3 mJ/m^2) and the residual water in the latex spheres remarkably decrease the T_g of polymer,[27] both can make polymer chains easily diffuse cross boundary of spheres and fill into the voids between the silica beads and cover the top layer of the film as well. As a result, the silica particles were embedded in the polymer chains and the small pores generated in the center of the polymer spheres (see Figure 9c). As the diffusion of chains continues, the pore becomes larger and the wall of the pores thinner; finally, the open cells form at the top layer of the film (see Figure 9d). As the water continues to evaporate, the second layer of spheres assembles under the first layer with silica particles filling in the interspaces, and the diffusion of the polymer chains generates pores in the center of the polymer spheres as the first layer of ordered porous structure forms. As the water continues to evaporate, the free surface of the wet film descends toward the substrate, the pores form layer by layer, and finally, the three-

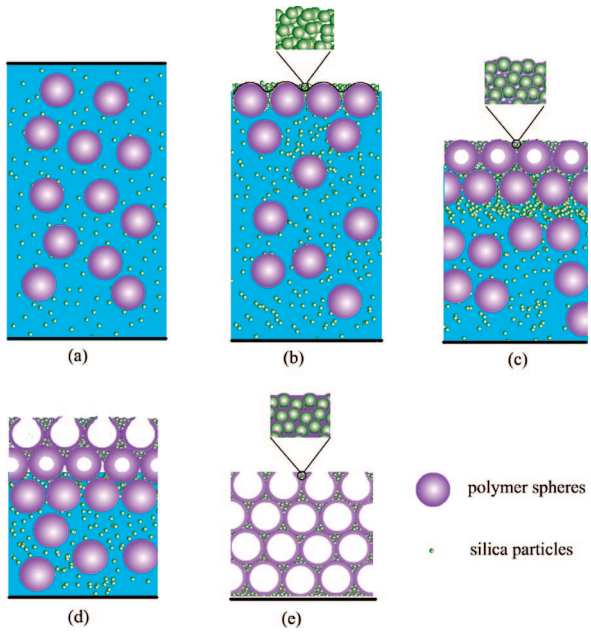

Figure 9. Diagram of formation mechanism of three-dimensional ordered porous film: (a) initial dispersion layer, (b) formation of colloidal crystal layer at the top surface, (c) generation of small pores in the center of the polymer spheres, (d) formation of open cells at the top layer and the second-layer assembly, and (e) final ordered porous film.

dimensional ordered porous structure is built, as shown in Figure 9e.

Conclusion

On the basis of this study, when the water-borne nanocomposite latex of monodisperse polymer spheres and colloidal silica particles is forced dry at comparatively high temperatures without predrying at ambient temperature, a three-dimensional ordered porous structure can be directly obtained; neither complex processes nor removal of any templates is needed. Therefore, it is really feasible, inexpensive, and environmentally friendly. More importantly, this process can be used for a large-scale fabrication of ordered porous polymer films with various polymer compositions and glass transition temperatures. However, the strong repulsive force between polymer sphere and colloidal silica particles is necessary to successfully prepare the stable nanocomposite latex and then the ordered porous film, and with too high T_g or too big polymer spheres, the film formation conditions need to be optimized to obtain this ordered porous structure.

The wet composite film dries starting from the top surface, and both the concave capillary bridge between particle pairs and electrostatic repulsion force push the polymer spheres to self-assemble into the first continuous layer of the ordered packed structure on the top surface. Meanwhile, the polymer chains easily diffuse across the boundary of spheres and fill into the voids between the silica beads, forming the first layer of the ordered porous structure. As the water continues to evaporate, the ordered particles array and then the ordered pores array form layer by layer, and finally the three-dimensional ordered porous structure is caused. This technique presents a new paradigm in the high-volume production of ordered porous polymer films that could be used for photonic crystals, biosensors, templates, catalysis, size- and shape-selective separation media, and so on.

Acknowledgment. Financial support from the Foundation of Science and Technology of Shanghai (07DJ14004), the NSF (No. 20774023), the Shanghai Leading Academic Discipline Project (B113), the Shanghai Excellent Leader of Academic Discipline Project, and the Shuguang Scholar-Tracking Foundation of Shanghai is appreciated.

References and Notes

(1) Harold, M. P.; Lee, C.; Burggraaf, A.77; J., K. Keizer; Zaspalis, V. T.; de Lange, R. S. A. *MRS Bull.* **1994**, *19*, 34–39.
(2) Bhave, R. R. *Inorganic Membranes Synthesis, Characteristics, and Applications*; Van Nostrand Reinhold: New York, 1991.
(3) Wu, M.; Fujiu, T.; Messing, G. L. *J. Non-Cryst. Solids* **1990**, *121*, 407–412.
(4) Litovsky, E.; Shapiro, M.; Shavit, A. *J. Am. Ceram. Soc.* **1996**, *79*, 1366–1376.
(5) Subramanian, G.; Manoharan, V. N.; James, D. T.; David, J. P. *Adv. Mater.* **1999**, *11*, 1261–1265.
(6) Geoffrey, I. N. W.; James, B. M.; Hicham, I.; Sun-Waterhouse, D. *Chem. Mater.* **2008**, *20*, 1183–1190.
(7) Xu, X.; Goponenko, A. V.; Asher, S. A. *J. Am. Chem. Soc.* **2008**, *130*, 3113–3119.
(8) Holland, B. T.; Blanford, C. F.; Stein, A. *Science.* **1998**, *281*, 538–540.
(9) Fan, J.; Deng, J.; Xing, C.; Yang, W. *J. Polym. Sci. Part A: Polym. Chem.* **2006**, *44*, 653–658.
(10) Yan, F.; Goedel, W. A. *Chem. Mater.* **2004**, *16*, 1622–1626.
(11) Stenzel, M. H.; Barner-Kowollik, C.; Davis, T. P. *J. Polym. Sci. Part A: Polym. Chem.* **2006**, *44*, 2363–2375.
(12) Zhang, Y.; Wang, C. *Adv. Mater.* **2007**, *19*, 913–916.
(13) Barner-Kowollik, C.; Dalton, H.; Davis, T. P.; Stenzel, M. H. *Angew. Chem., Int. Ed.* **2003**, *42*, 3664–3668.
(14) Meng, Y.; Gu, D.; Zhang, F.; Shi, Y.; Yang, H.; Li, Z.; Yu, C.; Tu, B.; Zhao, D. *Angew. Chem., Int. Ed.* **2005**, *44*, 7053–7059.
(15) Magbitang, T.; Lee, V. Y.; Cha, J.; Wang, H.; Chung, W.; Miller, R. D.; Dubois, G.; Volksen, W.; Kim, H. C.; Hedrick, J. L. *Angew. Chem., Int. Ed.* **2005**, *44*, 7574–7580.
(16) Norris, D. J.; Arlinghaus, E. G.; Meng, L. L.; Heiny, R.; Scriven, L. E. *Adv. Mater.* **2004**, *16*, 1393–1399.
(17) Holland, B. T.; Blanford, C. F.; Do, T.; Stein, A. *Chem. Mater.* **1999**, *11*, 795–805.
(18) Schroden, R. C.; Al-Daous, M.; Blanford, C. F.; Stein, A. *Chem. Mater.* **2002**, *14*, 3305–3315.
(19) Wang, J.; Li, Q.; Knoll, W.; Jonas, U. *J. Am. Chem. Soc.* **2006**, *128*, 15606–15607.
(20) Wang, Y.; Tang, Y.; Ni, Z.; Hua, W.; Yang, W.; Wang, X.; Tao, W.; Gao, Z. *Chem. Lett.* **2000**, *29*, 510–511.
(21) Huang, L.; Wang, Z.; Sun, J.; Miao, L.; Li, Q.; Yan, Y.; Zhao, D. *J. Am. Chem. Soc.* **2000**, *122*, 3530–3531.
(22) You, B.; Wen, N.; Zhou, S.; Wu, L.; Zhao, D. *J. Phys. Chem. B.* **2008**, *112*, 7706–7712.
(23) You, B.; Shi, L.; Wen, N.; Liu, X.; Wu, L.; Zi, J. *Macromolecules.* **2008**, *41*, 6624–6626.
(24) Holl, Y.; Keddie, J. L.; McDonald, P. J.; Winnik, W. A. *Film Formation in Coatings: Mechanisms, Properties and Morphology*; Provder, T., Urban, M. W. Eds.; ACS Symposium Series 790; American Chemical Society: Washington, DC, 2001; Chapter 1, pp 2−26.
(25) Dimitrov, S.; Nagayama, K. *Langmuir* **1996**, *12*, 1303–1311.
(26) Stamou, D.; Duschl, C.; Johannsmann, D. *Phys. Rev. E* **2000**, *62*, 5263–5272.
(27) Song, M.; Hourston, D. J.; Silva, G. G; Machado, J. C. *J. Polym. Sci. Part B: Polym. Phys.* **2001**, *39*, 1659–1664.

MA900055F